

Crystallization of Highly Soluble Thioglucopyranoside Ejected by Coherent Molecular Vibrational Excitation using a Visible 10-fs Pulsed Laser

Izumi Iwakura,^{*a,b} Sena Hashimoto,^b Kotaro Okamura,^b Keiko Komori-Orisaku,^b Shoji Akai,^b
Atsushi Yabushita^b

^a *Department of Chemistry, Faculty of Engineering, Kanagawa University,
3-27-1 Rokkakubashi, Yokohama 221-8686, Japan*

^b *Research Institute of Engineering, Kanagawa University, 3-27-1 Rokkakubashi, Yokohama 221-
8686, Japan*

Contents

| | |
|---|----|
| Section S1. X-ray Single-Crystal Structural Analysis of BHPTG | 2 |
| Section S2. ¹ H NMR Analysis of BHPTG | 4 |
| Section S3. Raman Spectra | 5 |
| Section S4. Data for Confirmation of Reproducibility | 6 |
| Section S5. Stabilization System for the Visible 10-fs Pulsed Laser | 9 |
| References | 11 |

Section S1. X-ray Single-Crystal Structural Analysis of BHPTG

Single crystals of BHPTG, formed by sublimation on the wall of the glass cell, were suitable for X-ray analysis. The colourless crystals were coated with paraffin oil, mounted with Micromount (Mitegen), and then immediately cooled at 93 K in cool nitrogen gas. All measurements were obtained on a VariMax Dual (RIGAKU) Saturn724 diffractometer using multilayer mirror monochromated Mo-K α radiation. Diffraction data were processed using the CrystalClear package^{S1}. The crystal structure was solved by direct methods (SIR 2002)^{S2} and refined by the full-matrix least-squares method on F² using SHELXL-2014^{S3} (Fig. S1 and Tables S1). The positions of the hydrogen atoms in water molecules were refined using isotropic displacement parameters that restrained the bond lengths. Selected crystal data and structure refinement details are presented in Table S1. All H atoms were positioned geometrically and treated as travelling on their parent atoms. The CCDC reference number is 1884023.

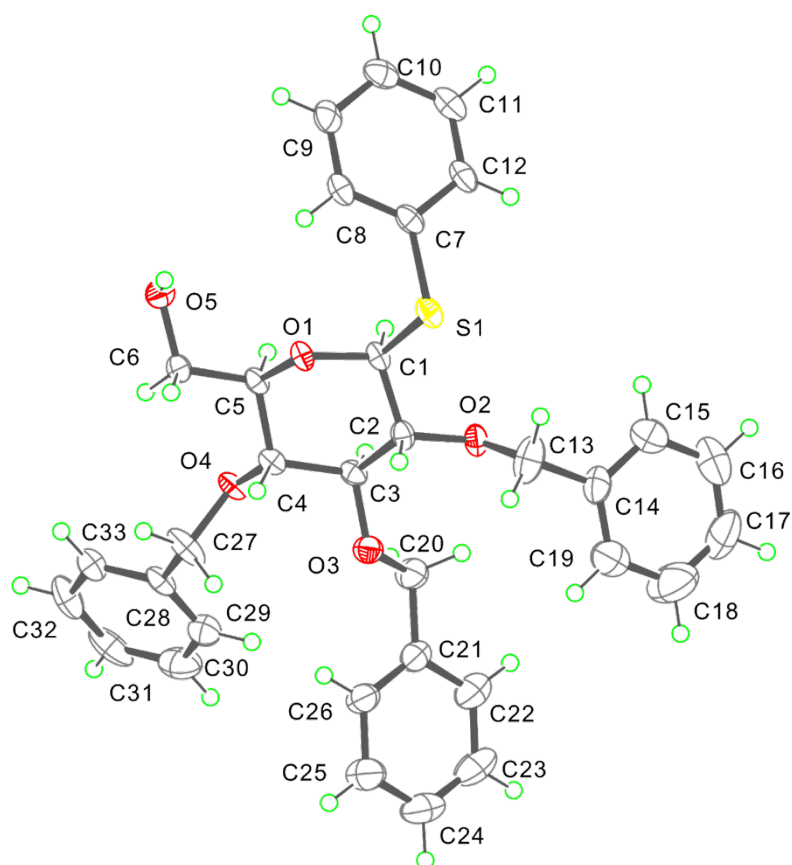


Figure S1. Crystal structure of 2,3,4-tri-*O*-benzyl-6-hydroxy-1-phenylthio- β -D-glucopyranoside (BHPTG). Displacement ellipsoids are drawn at the 50% probability level. Grey, blue, red, yellow and green spheres represent C, N, O, S and H atoms, respectively.

Table S1. Crystal Data and Refinement Parameters of BHPTG

| | | | |
|--|---|--|---------------|
| Crystal data | Formula | C ₃₃ H ₃₄ O ₅ S | |
| | Mr | 542.66 | |
| | λ / Å | 0.71075 | |
| | crystal system | monoclinic | |
| | space group | P2 ₁ | |
| | T / K | 93(2) | |
| | a / Å | 13.5003(8) | |
| | b / Å | 4.5570(3) | |
| | c / Å | 23.5269(17) | |
| | β / deg | 102.166(7) | |
| | V / Å ³ | 1414.89(17) | |
| | Z | 2 | |
| | μ (Mo K α) / mm ⁻¹ | 0.155 | |
| | $F(000)$ | 576 | |
| | crystal size / mm ³ | 0.166 x 0.02 x 0.01 | |
| | Data collection | T_{\min} , T_{\max} | 0.835, 1.000 |
| | | θ_{\min} , θ_{\max} / deg | 2.583, 27.500 |
| No. of total reflns | | 11368 | |
| No. of unique reflns (R_{int}) | | 6187 (0.0459) | |
| No. of obsd reflns [$I \geq 2\sigma(I)$] | | 5028 | |
| Refinement | $R1$, $wR2$ [$I > 2\sigma(I)$] | 0.0590, 0.1393 | |
| | $R1$, $wR2$ (all data) | 0.0783, 0.1498 | |
| | GOF | 1.06 | |
| | No. of parameters | 353 | |
| | $\Delta\rho$ / eÅ ³ | 0.469, -0.312 | |
| | Frack parameters | 0.15(6) (1697 Friedel pairs) | |

Section S2. ^1H NMR Analysis of BHPTG

The ^1H NMR spectra were recorded using NMR spectrometers (JEOL, JNM-ECA-500 and 600) in chloroform- d referenced to tetramethylsilane (0.00 ppm).

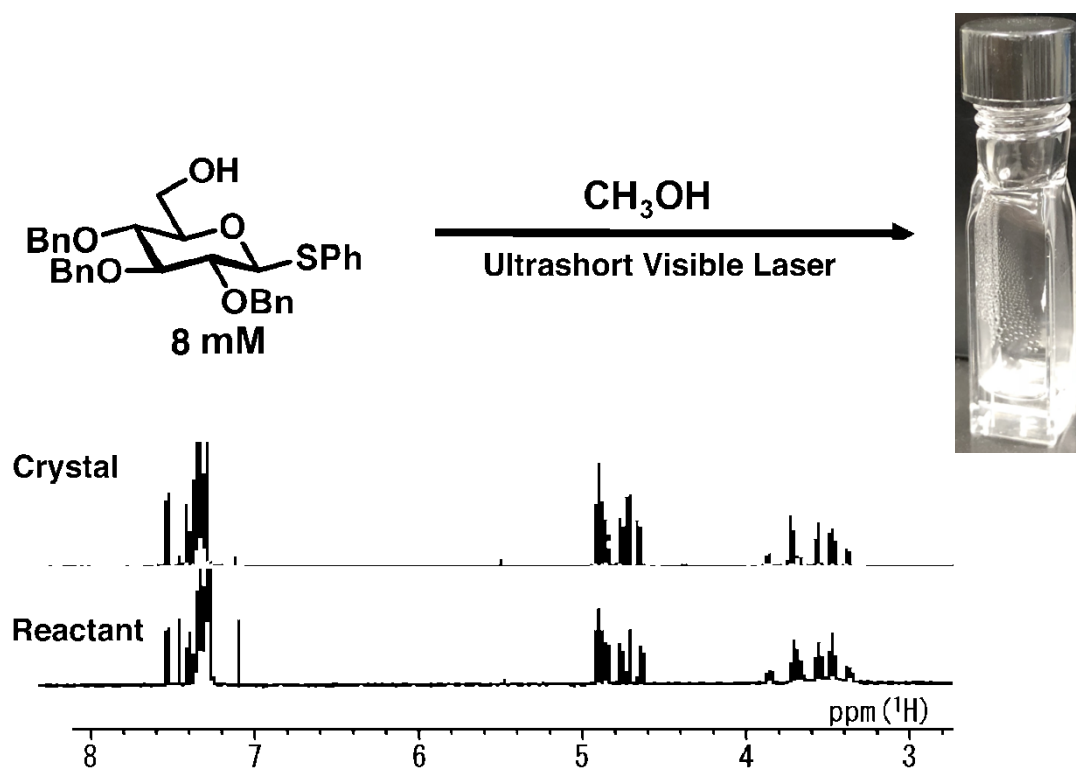


Figure S2. ^1H -NMR spectra of the reactant and crystals sublimed from a methanol solution of BHPTG.

Section S3. Raman Spectra

The Raman spectra of BHPTG (solid sample), methanol (liquid sample), and acetonitrile (liquid sample) were measured using a Raman spectrometer (JASCO, RMP-320) under 532-nm laser excitation.

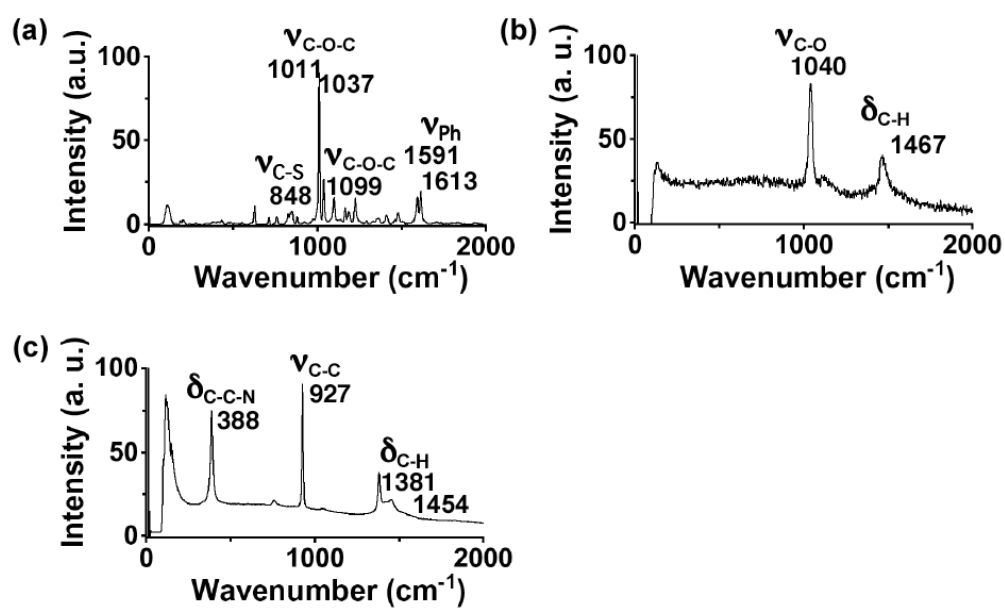


Figure S3. Raman spectra generated from excitation with a 532-nm laser. (a) BHPTG, (b) methanol, and (c) acetonitrile.

Section S4. Data for Confirmation of Reproducibility

For the crystal deposition experiment, we used a screw-capped glass cell whose inner wall was coated with Si to a level up to 20 mm from the bottom of the cell. The Si coating avoided the liquid level rise caused by surface tension. The internal surface of the glass cell was coated with dichlorodimethyl silane (TCI Inc.), then washed in toluene. The washed glass cell was placed upside down, and the upper part of the glass cell was dipped in 1 N NaOH aqueous solution overnight to remove the Si coat. Then, the glass cell was washed in water after it was neutralized by soaking in nitric acid. Since the meniscus of water was convex in the upward direction, it was confirmed that a Si coat had formed on the internal surface. When the BHPTG solution stored in the Si-coated glass cell was left at room temperature for one day, no crystals were deposited in the glass cell.

The experimental results are summarized in Table S2, which shows that crystal deposition had no dependence on the polarization or laser intensity. The irradiation intensity threshold for ablation in solution was reported to be dependent on compound type and within the range of 5-30 mJ/cm² using YAG laser (center wavelength 355 nm, pulse duration 7 ns, repetition rate 10 Hz) and excimer laser (center wavelength 351 nm, pulse duration 30 ns, repetition rate 5 Hz)^{S4}. In the present work, crystals were found to be deposited even with irradiation intensities as low as 0.2 mJ/cm². Therefore, the crystals deposited on the glass wall in the present work were not likely formed from aerosols produced by laser ablation, even though the possibility of laser ablation cannot be completely ruled out.







The crystal was typically deposited on the glass wall opposite to the irradiated side. The place where the crystal was deposited is marked by a pink circle, and the direction of the laser irradiation is shown by orange arrows in Table S2. The irradiation time required to obtain a visible amount of deposited crystal was different for each experiment.

Table S2. Crystal deposition reproducibility for a methanol solution of BHPTG in a quartz glass rectangular cell (the laser was pulsed with repetition rate of 1000 Hz).

| Solvent | Concentration (mol L ⁻¹) | Laser Polarization | Irradiation Power (mJ cm ⁻²) | Irradiation Time ^{a)} (h) | Deposited Place | Number of Trial | Number of Trial with Crystal | Nucleation Efficiency (%) |
|--------------------|--------------------------------------|--------------------|--|------------------------------------|-----------------|-----------------|------------------------------|---------------------------|
| CH ₃ OH | 1.5 | Horizontal | 27 | 25 (9) | | 3 | 3 | 100 |
| | | | 27 | 25 (-) | | | | |
| | | Vertical | 21 | 25 (21) | | | | |
| | 3.0 | Horizontal | 24 | 46 (20) | | 4 | 4 | 100 |
| | | | 25 | 22 (-) | | | | |
| | | Vertical | 18 | 48(28.5) | | | | |
| | | | 20 | 20 (-) | | | | |
| | 5.5 | Horizontal | 0.3 | 15 (3.5) | | 13 | 9 | 69 |
| | | | 0.4 | 25 (-) | | | | |
| | | | 0.4 | 8 (-) | | | | |
| | | | 3 | 48 (3.5) | | | | |
| | | | 3 | 48 | | | | |
| | | | 19 | 9 (-) | | | | |
| | | | 22 | 48 | | | | |
| | | | 26 | 7 (-) | | | | |
| 27 | | | 4 (-) | | | | | |
| 29 | | | 28 | | | | | |
| 30 | | | 9 (-) | | | | | |
| Vertical | | 0.2 | (15) | | | | | |
| 2 | 48 | | | | | | | |
| 8 | Horizontal | 28 | 12 (-) | | 1 | 1 | 100 | |
| CH ₃ CN | 8 | Horizontal | 20 | 48 | | 4 | 0 | 0 |
| | 11 | Horizontal | 23 | 48 | | | | |
| | 39 | Horizontal | 23 | 48 | | | | |
| | | Vertical | 18 | 48 | | | | |

a) The number in parentheses shows the time when the deposited crystal began to be visible. When the crystal was already visible within an hour of irradiation time, the time is shown as (-). Even after the crystal became visible, the solution was irradiated to deposit sufficient crystals for NMR analysis.

Table S3. Crystal deposition reproducibility for a methanol solution of BHPTG in a quartz glass rectangular cell (the laser was pulsed at repetition rate of 500 Hz).

| Solvent | Concentration (mol L ⁻¹) | Laser Polarization | Irradiation Power (mJ cm ⁻²) | Irradiation Time (h) | Deposited Place | Number of Trial | Number of Trial with Crystal | Nucleation Efficiency (%) |
|---------|--------------------------------------|--------------------|--|----------------------|--|-----------------|------------------------------|---------------------------|
| | 5.5 | Horizontal | 22 | 48 ^{a)} |  | 6 | 6 | 100 |
| | | | 16 | 8 |  | | | |
| | | | 16 | 13 |  | | | |
| | | Vertical | 16 | 48 ^{a)} |  | | | |
| | | | 12 | 8 |  | | | |
| | | | 12 | 13 |  | | | |

a) Deposited crystals that became visible after irradiation for 48 hours disappeared after irradiation for 60 hours.

Section S5. Stabilization System for the Visible 10-fs Pulsed Laser

Because of daily temperature variations of approximately 1 degree Celsius peak-to-peak, the NOPA (see Fig. S4, NOPA Optical Layout) output varied up to the total extinction in experimental sessions. For continuous irradiation experiments of several tens of hours, we stabilized the NOPA output by feedback systems.

The NOPA amplifies seed white light by parametric amplification pumped with the second-harmonic (SHG) pulse (NOPA-pump, centre wavelength 400 nm) of a Ti:sapphire regenerative amplifier output NIR pulse (pulse duration 100 fs, centre wavelength 800 nm). The seed white light is also generated from one split-out beam of the same NIR pulse by self-phase modulation in a sapphire plate ("Sa").

The stabilization systems are implemented as two independent proportional-integral-differential (PID) controllers, partly following our past work^{S5}. One controller stabilizes the NOPA-pump energy (detection with "PD₁"), and the other stabilizes the 800 nm pulse energy for seed white-light generation ("PD₃"). The latter controller (NOPA-seed) is different from past work, which directly stabilized the seed white-light pulse energy after an 800 nm blocking filter.

Pulse-energy detection is achieved with Si PIN photodiodes (Hamamatsu Photonics), and their photocurrent signals after passing through homemade low-pass filters and impedance-matching amplifiers are digitized by USB-DAQ (National Instruments USB6009). PID controllers are implemented with a unified LabVIEW program on a personal computer. The PID actuators are stepping motor-driven rotation stages (Sigma-Koki SGSP-40).

The stabilization of NOPA-pump involves rotating the half-wave plate ("HWP") just before the crystal for SHG. The rotation around the beam path changes the beam polarization after the HWP, effectively modulating the SHG efficiency and NOPA-pump (400 nm) pulse energy. NOPA-pump is reflected by three 400 nm reflection/800 nm transmission mirrors ("M₂"-"M₄", harmonic separators) to remove unconverted 800 nm light. For pulse-energy detection, the sample beam is split off by a microscope cover glass and reflected once by a harmonic separator ("M₅") for further selection of the 400 nm component before being incident upon the photodiode ("PD₁").

The stabilization of NOPA-seed involves rotating a circular variable reflective neutral-density filter ("VND₂", Sigma-Koki VND-100) before the sapphire plate for white-light generation. The sample beam for pulse-energy detection is simply split off by a microscope cover glass after neutral-density filtering and is incident upon the photodiode ("PD₃").

The PID time constants are deliberately set for sluggish movement, eliminating unwanted responses to air turbulence and restricting the system to only counting laser intensity fluctuations caused by hour-long room-temperature changes.

The stabilization realized continuous output of the NOPA for 72 hours as shown in Fig. S5 where x-axis, y-axis, and grayscale represent time, laser wavelength, and laser intensity, respectively.

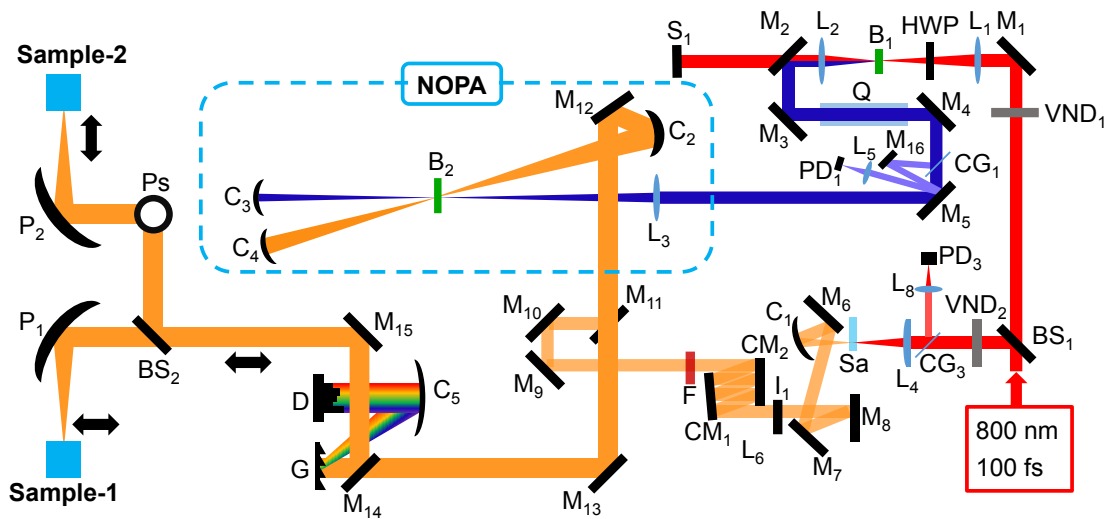


Figure S4. Schematic diagram of the laser system. BS: Beam Splitter, VND: Variable Neutral Density Filter, M: Mirror, L: Convex Lens, HWP: Half-Wave Plate, B: BBO Crystal, S: Beam Stop, Q: Quartz Block, CG: Cover Glass, PD: Photodiode, Sa: Sapphire Plate, I: Iris, C: Concave Mirror, CM: Chirped Mirror, F: Short-Pass Filter, G: Grating, D: Deformable Mirror, P: Parabolic Mirror, Ps: Periscope, Red line: 800-nm Pulse, Blue line: SHG 400-nm Pulse, Orange line: White-light Pulse.

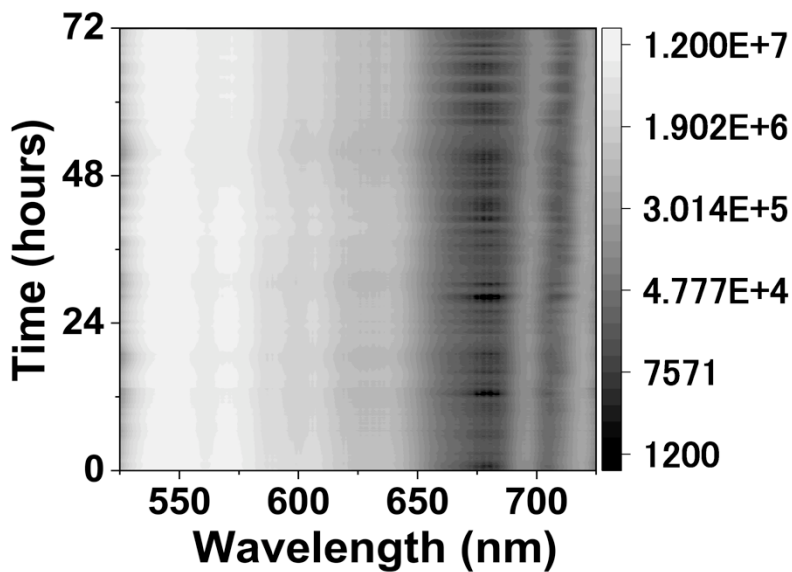


Figure S5. Stabilized output of the NOPA.

References

- S1. Rigaku (2010). CrystalStructure. Version 4.0. Rigaku Corporation, Tokyo, Japan.
- S2. M. C. Burla, M. Camalli, B. Carrozzini, G. L. Cascarano, C. Giacovazzo, G. Polidori, R. Spagna, *J. Appl. Cryst.* **2003**, *36*, 1103.
- S3. G. M. Sheldrick, *Acta Cryst.* **2015**, *C71*, 3.
- S4. Masuhara, H, *Bull. Chem. Soc. Jpn.* **2013**, *86*, 755.
- S5. K. Okamura and T. Kobayashi, *Jpn. J. Appl. Phys.*, **2009**, *48*, 070214.